Available online at www.sciencedirect.com
ScienceDirect
International Journal of Mass Spectrometry 255–256 (2006) 232–238
International Journal of Mass Spectrometry
www.elsevier.com/locate/ijms

Single, double and triple ionization of tetraphenyl iron(III) porphyrin chloride

S. Feil [a], M. Winkler [a], P. Sulzer [a], S. Ptasinska [a], S. Denifl [a], F. Zappa [a], B. Kräutler [b], T.D. Märk [a,1], P. Scheier [a,*]

[a] *Institut für Ionenphysik und Angewandte Physik, Leopold-Franzens Universität Innsbruck, Technikerstr. 25, A-6020 Innsbruck, Austria and Centre of Molecular Biosciences Innsbruck, Austria*
[b] *Institut für Organische Chemie, Leopold-Franzens Universität Innsbruck, Innrain 52, A-6020 Innsbruck, Austria and Centre of Molecular Biosciences Innsbruck, Austria*

Received 11 December 2005; received in revised form 19 January 2006; accepted 19 January 2006
Available online 28 February 2006

Abstract

Tetraphenyl iron(III) porphyrin chloride (FeTPPCl) cations are generated in the gas phase by electron impact ionization. The ionization is accompanied by extensive fragmentation as well as formation of doubly and triply charged ions. The most prominent fragments are analyzed and identified by fitting with calculated natural isotope patterns. Appearance energies of the most abundant singly and doubly charged product ions are determined. For the singly charged parent ions $FeTPPCl^+$, $CuTPP^+$ and the fragment ion $FeTPP^+$ we obtain a value of 9.7 ± 0.5 eV which is about 3 eV higher than the value published for photo ionization of FeTPPCl. The appearance energy of the doubly charged ion $FeTPP^{2+}$ is obtained to be 18 eV. The additional loss of one or two phenyl groups requires between 10 and 14 eV more for singly and doubly charged ions. Also, the metastable decay of singly and doubly charged ions is investigated with the mass analyzed ion kinetic energy (MIKE) scan technique, performed on a three sector field mass spectrometer (BEE-geometry). In the mass spectrum and the MIKE scans a strongly reduced stability of the porphyrin ions is observed with increasing charge state.

Keywords: Electron impact ionization; Multiply charged ions; Porphyrins; Unimolecular dissociation

1. Introduction

Porphyrins, the "pigments of life" are perhaps the most important and widespread class of natural pigments [1]. Nature provides a variety of tetrapyrrolic pigments with a similar ligand core, but differing in the metal centre and the side groups attached to the porphyrin rings. For instance, in heme (the prosthetic group in haemoglobin) the metal centre is an iron ion, in the case of chlorophyll it is magnesium and in vitamin B_{12} it is cobalt [2,3]. Porphyrins are not only of prime importance in a large variety of biological processes, but also in chemical catalysis and as geological markers. Porphyrins are also used for tumor localization (as biomarkers) and in photodynamic tumor treatments [4]. Identification of porphyrins present in biosystems or deposited in tissues is used to diagnose a number of metabolic abnormalities [5]. Synthetic porphyrins have been used extensively to investigate single electron transfer reactions of natural biological processes [6] such as photosynthesis [7]. In addition, the identification and characterisation of porphyrins that occur in fossil fuels (geoporphyrins) [8] is often desirable. For example, geoporphyrins are used as biomarkers to estimate the age of petroleum source rocks because their carbon skeletons are preserved through geological time [9,10]. With their remarkable chromophore structures and molecular symmetry metal porphyrins are also of considerable theoretical interest in their own right to physicists and chemists [2]. The tetraphenyl porphyrins are chemically robust and a group of easily prepared, symmetrical porphyrins [11]. Therefore they are frequently used as models for the more complex natural porphyrinoids.

Mass spectrometry has proven to be an important tool for the analysis of porphyrins, especially the more volatile and robust

* Corresponding author. Fax: +43 512 507 2932.
E-mail address: Paul.Scheier@uibk.ac.at (P. Scheier).
[1] Also Adjunct Professor at Department of Plasmaphysics, Comenius University, SK-84248 Bratislava, Slovak Republic.

1387-3806/$ – see front matter © 2006 Elsevier B.V. All rights reserved.
doi:10.1016/j.ijms.2006.01.032

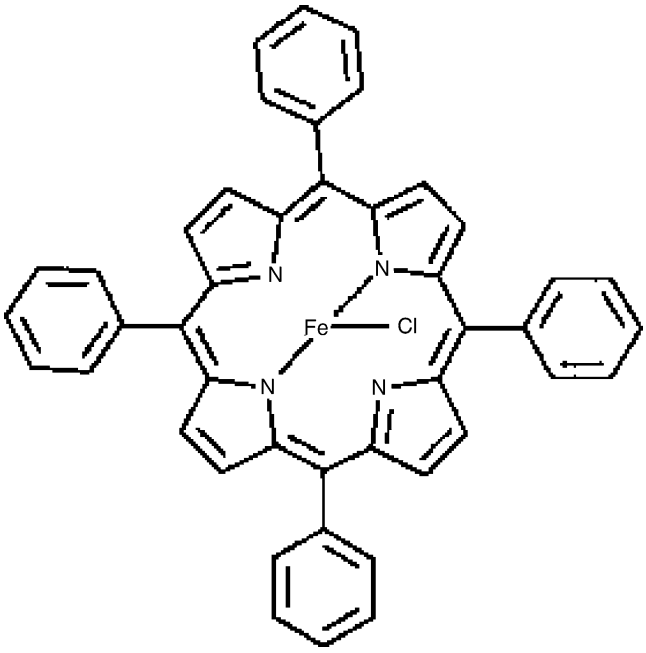

Fig. 1. Structure of the tetraphenyl iron(III) porphyrin chloride (FeTPPCl) molecule.

porphyrins [12]. Electron impact ionization mass spectra are generally characterized by a singly charged molecular ion as the base peak and relatively abundant singly and doubly charged fragment ions. There is generally no cleavage of the macrocycle nucleus. After ionization, the positive charge is localized essentially in the extended π system of the macrocycle, and therefore fragmentation occurs only by the degradation of substituents, which are fixed by the rigid ring system. Moreover the relative importance of even and odd electron systems (e.g., fragmentation originating from singly and doubly charged precursors) can be investigated under comparable experimental conditions. In the present work however, a specific kind of porphyrins is used, namely the tetraphenyl iron(III) porphyrin chloride (FeTPPCl). The core structure of this porphyrin is similar to the hemin (a derivate of the heme), but the side chains are different (see Fig. 1).

In this work we focus on the evaluation of the isotopically resolved mass spectra of singly, doubly and triply charged tetraphenyl iron(III) porphyrin chloride. Additionally, we determine the appearance energies of the most abundant singly and doubly charged fragment ions. Finally, we also investigate the stability of the ions in a metastable time regime with a mass analyzed ion kinetic energy (MIKE) scan technique.

2. Experimental

The experimental set-up and the data acquisition and analysis procedures have been described in detail in previous publications [13–15]. In brief, the apparatus consists of a high-resolution double-focusing mass spectrometer of reversed Nier–Johnson geometry in conjunction with a second electrostatic analyzer as shown schematically in Fig. 2. The FeTPPCl powder is evaporated in an oven at 300 °C. The produced porphyrin vapor is

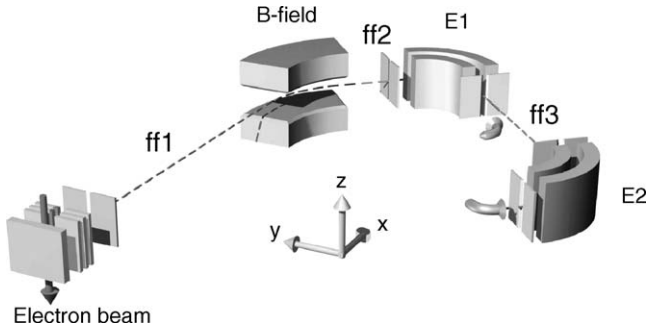

Fig. 2. Schematic view of the experimental set-up.

ionized by a well-characterized electron beam (70 eV electron energy, 1 eV electron energy spread and 300 μA electron current) in the Nier-type ion source and the cations are extracted from the collision chamber by a weak penetrating electric field and accelerated towards the mass spectrometer by a potential of 3 kV. The ions pass through a first field-free region (ff1), are momentum analyzed by the magnetic sector field (B), enter a second field-free region (ff2), pass through the first electrostatic analyzer (E1), and enter a third field-free region (ff3). In one mode of operation, a channeltron placed in ff3 detects all ions that emerge from the exit slit of the first electrostatic analyzer. In another mode of operation, the ions are allowed to traverse ff3, enter a second electrostatic analyzer (E2), and are finally detected by a channeltron at the exit of E2.

In the first mode of operation, mass analyzed ion kinetic energy (MIKE) spectra of ions of mass m_p and charge z_p selected by the magnetic sector field that undergo decay in ff2 into a specific final product ion of mass m_f and charge z_f (accompanied by other neutral and/or charged reaction products) are obtained by scanning the sector field voltage U of E1 and recording the intensity of the m_f, z_f ions as a function U. If the parent ions are transmitted by E1 at a sector field voltage U_p, the fragment ions formed in ff2 are transmitted at a sector field voltage U_f which is given by

$$U_f = U_p \frac{m_f/z_f}{m_p/z_p}. \quad (1)$$

In the second mode of operation, the decay of the ions is analyzed in ff3 by tuning the magnet and the electrostatic sector (E1) to transmit the stable parent ion. Subsequently, the sector field voltage of E2 is scanned. The magnetic field B and the first sector field E1 act as a double-focusing high-resolution mass spectrometer. As before, Eq. (1) applies.

The average kinetic energy release (<KER>) of a decay process under study can be determined from the MIKE scan as discussed in Ref. [15] to which we refer the reader for further details. For unimolecular dissociations in ff3 the interference of isotopes in the MIKE spectrum is strongly reduced because the first two sectors (B, E1) serve as a high-resolution double-focusing mass spectrometer. Thus the only interference results from dehydrogenated ions that contain one ^{13}C atom. According to analysis of the peak patterns such a contribution is less than 1% for the singly charged ions investigated.

For the measurement of the appearance energies of the interesting ions the electron current is kept low, i.e., about 10 μA, to assure single collision conditions during the ionization process and to avoid space charge effects at low electron energies.

3. Results and discussion

3.1. Mass spectra

The mass spectrum (Fig. 3) shows three distinct groups of ions: a high (*m*/*z*) group of singly charged ions, a medium *m*/*z* group of doubly charged ions and a low *m*/*z* group of triply charged ions. Singly charged fragment ions may also be present in the low and medium regions, but in the medium *m*/*z* region their relative abundance is very low. The production of small singly charged fragment ions is very improbable because of the unlikely break-up of the extremely stable macrocycle (the porphyrin ring). We cannot confirm the recent report by Laycock et al. [16] of scission of the porphyrin macrocycle in 5-nitro octaethylporphyrin. We observe no significant signal in the mass range of the macrocycle that has a *m*/*z* ratio of about 360 thomson.

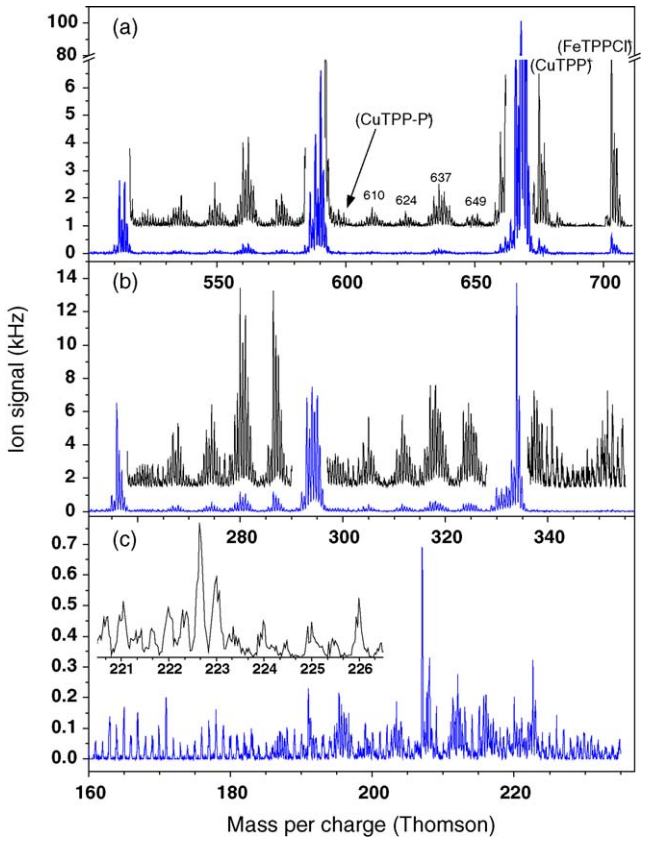

Fig. 3. Mass spectrum of FeTPPCl recorded at an electron energy of 70 eV. The electron current is around 300 μA and the oven temperature is set to 573 K resulting into an ion source pressure of 5×10^{-6} Pa. The upper diagram (Fig. 3a) shows the singly charged ions of the high *m*/*z* regime, in the middle (Fig. 3b), the doubly charged regime is presented and the lowest panel (Fig. 3c) shows the triply charged regime. In Fig. 3a and b the mass spectra, except for the high intensity peaks, are plotted a second time multiplied by a factor of 10 and added with a constant shift to see in more details the low-intensity peaks. The numbers in Fig. 3a indicate the mean mass of the corresponding bunch of peaks.

Fig. 3a shows an isotopically resolved mass spectrum in the high *m*/*z* region, recorded at electron energy of 70 eV, an oven temperature of 300 °C and a pressure in the ion source of 5×10^{-6} Pa. The parent cation has a nominal *m*/*z* ratio of 703 thomson. The most intense peak is found at *m*/*z* of 668 thomson and can be assigned to the dissociation of the parent ion ($C_{44}H_{28}N_4FeCl$) into Cl and $C_{44}H_{28}N_4Fe^+$ (FeTPP). The intense peaks at *m*/*z* 590 and 512 thomson correspond to the loss of one or two phenyl radicals and a hydrogen atom (perhaps two benzene molecules).

The various isotopes of the constituent atoms of FeTPPCl (C, Cl, Fe, N) result in a complex peak pattern around the nominal mass. The peak heights are in good agreement with the calculated natural isotopic pattern. Towards lower masses small deviations may arise from the loss of H atoms, i.e., for fragment cations intramolecular protonation or attachment of hydrogen atoms during the dissociative ionization reaction from the opposite fragments may lead to an increase of the ion yield of the peaks at higher masses. For a quantitative analysis of the structure and the composition of the peaks, a fitting procedure is performed. The measured group of peaks is fitted with the calculated isotope pattern for a certain mass to charge ratio. For example, the nominal mass of the parent ion $C_{44}H_{28}N_4FeCl^+$ is 703 and the corresponding isotopomers span the range from 701 to 707 thomson. A computer program fits the measured mass distribution with a superposition of calculated isotopic patterns that are shifted by some masses to the left and to the right, assuming that loss or addition of H atoms does not change the isotope patterns. This analysis is performed for the most abundant peaks at nominal mass to charge ratios of 668 [$(FeTPP)^+$], 590 [$(FeTPP - P)^+$] and 512 thomson [$(FeTPP - 2P)^+$] and the corresponding doubly charged fragments at mass to charge ratios of 334 [$(FeTPP)^{2+}$], 295 [$(FeTPP - P)^{2+}$] and 256 thomson [$(FeTPP - 2P)^{2+}$]. Where −P and −2P indicate the number of phenyl groups that are lost. The results can be seen in Fig. 4a. In case of the most prominent peak at *m*/*z* ratio of 668 thomson we conclude that more than 94% of the signal is originating from the natural isotopic pattern of the $FeTPP^+$. About 3% and 1.8% of the signal are resulting from the loss of 2 or 4 hydrogen atoms (or 1 or 2 hydrogen molecules), respectively. Other decay channels such as the loss of an odd number of H atoms play just a minor role. The left-hand side of Fig. 4a shows the most prominent singly charged fragments and the corresponding doubly charged ions are shown on the right-hand side. In comparison to the singly charged fragment ions the corresponding doubly charged ions exhibit a peak pattern that is clearly shifted to lower masses and this indicates additional loss of H atoms. The detailed composition of the peaks is listed in Table 1. An additional shift to lower masses is observed with the number of the phenyl groups that are lost. It is also interesting to note that in case of a phenyl loss the most abundant peak is never the ion that is generated via a simple C–C_6H_5 bond cleavage and the loss of C_6H_5 but that resulting from the additional loss of an H atom. Apparently intact benzene molecules C_6H_6 are detached following an intramolecular rearrangement. The only exception

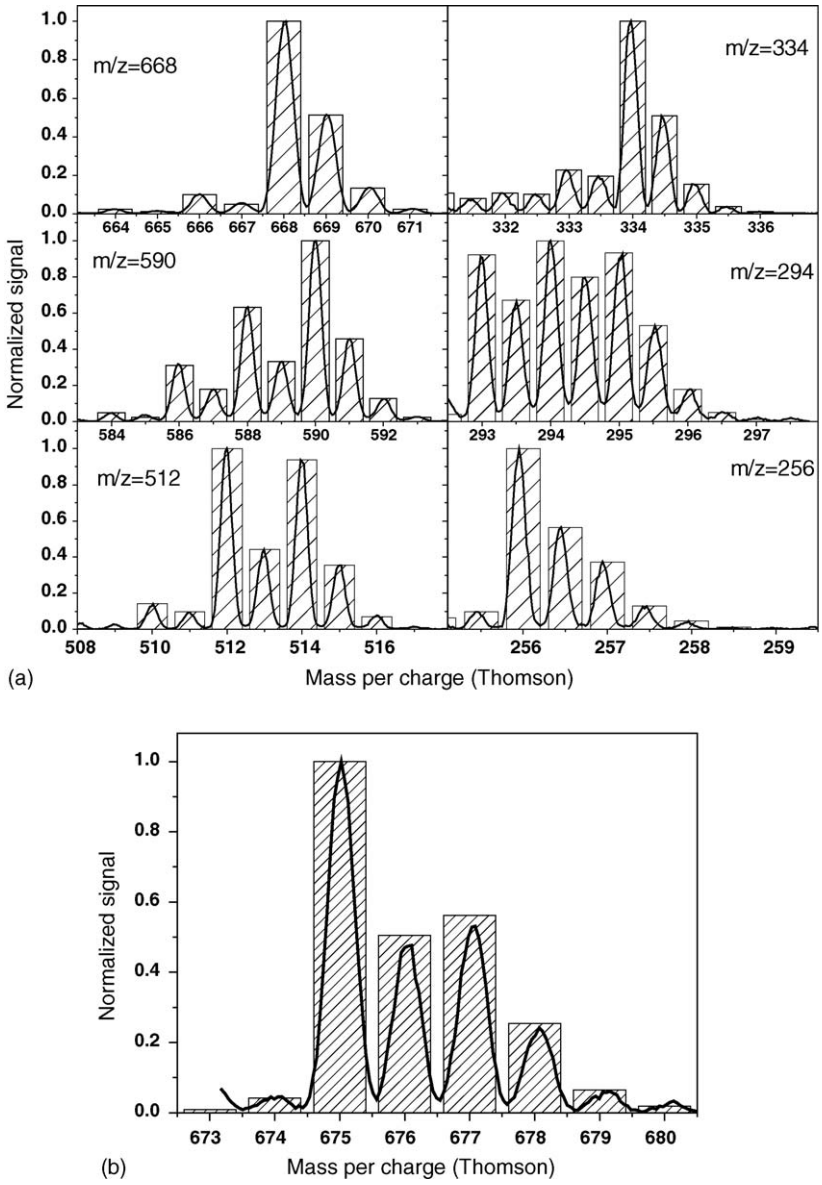

Fig. 4. (a) Mass spectra of the most abundant singly (left-hand side) and doubly-charged (right-hand side) fragments (solid lines) fitted with calculated natural isotopic patterns (hatched bars). Also given is the *m*/*z* ratio of the most abundant mass peak. (b) Mass spectrum of an impurity at 675 thomson (solid line) fitted with a calculated natural isotopic pattern of the molecule tetraphenyl copper porphyrine CuTPP.

Table 1
Detailed composition of the peaks as shown in Fig. 4

	Singly charged *m*/*z* abundance (%)				Doubly charged *m*/*z* abundance (%)		
	675	668	590	512	334	294	256
	93.7	92.4	48.1	46.8	64.9	21.3	65.3
−H	3.5		3	2	6.4	12.6	4.4
−2H	0.7	3.2	27.8	4.1	9	24.1	
−3H	0.2		1.9		3.4	7.5	
−4H		1.8	14.4		5	27.7	
−5H					1.5		
−6H			1.6		7		
+H			1.5	3.1		5.7	12.5
+2H			1	42.7	1.5	0.7	15.5
+3H	1.8			0.8		0.4	1.1
+4H							1.3

is the loss of two C_6H_5 units (probably combined into a bicyclic structure) from the singly charged FeTPP which has almost the same probability as the loss of two benzene molecules.

A series of peaks at $m/z = 675$ thomson (Fig. 4b) has the nominal mass of $C_{44}H_{28}N_2FeCl$ (parent-N_2). However, an analysis of the isotope pattern and the presence of this peak also in the mass spectrum of negative ions indicate that this ion is not a fragmentation product but rather an impurity caused by $C_{44}H_{28}N_4Cu$ (CuTPP). This impurity also appears at the m/z ratio of 597 which indicates the loss of one phenyl group together with one H atom (benzene). Moreover it is also visible in the doubly charged regime (inset in Fig. 3b). A likely source for this impurity is an exchange of iron with copper from the walls of the oven in which the powder is evaporated. The size of this peak strongly depends on the area of the copper containing parts of the oven.

Dications are observed in the m/z range between about 250 and 350 thomson (Fig. 3b). Please note that the mass ranges representing the doubly and triply charged regimes are chosen in a way that the same ions in different charge states are lining up at the same position relative to the x-axis. Although it is sometimes difficult to unequivocally assign peaks to doubly charged ions we are certain about our assignment since every second peak is at a half integer mass to charge ratio. The most abundant dications are the doubly charged fragments that correspond to the most abundant singly charged fragment ions, i.e., FeTPP and FeTPP minus one and two phenyl groups ($FeTPP - P$, $FeTPP - 2P$), respectively. The detailed composition of the peaks can be seen in Fig. 4a. The triply charged regime is presented in Fig. 3c. The triply charged ions are easily identified because the peaks are situated at a third of a mass unit. The inset of Fig. 3c shows the section around the triply charged FeTPP. Above a mass to charge ratio of 224 thomson only singly and doubly charged ions are present. The relative abundance of the triply charged ions is clearly dominating the mass spectrum between 195 and 224 thomson. The signal in this regime is too low for a further analysis of the peak patterns. Between the $FeTPP^{3+}$ and the $(FeTPP - P)^{3+}$ ion we observe a series of triply charged fragment ions. However, there is no indication of the existence of the $(FeTPP - 2P)^{3+}$.

Our results are in good agreement with findings from other groups working with laser photoionization (193 nm) on hemin [17]. They also found that the fragment ion formed in the dissociation process of the parent FeTPPCl into mass to charge ratio 668 thomson $(FeTPP - Cl)^+$ and Cl is more abundant than the parent. Furthermore, they also identified the losses of phenyl rings + H (probably benzene) at m/z ratios of 590 and 512 thomson.

The peaks with even mass to charge ratios are in general higher than the ones with odd ratios. Between the prominent peaks at 668 thomson and 590 thomson one can observe a more or less regular structure of peaks every 12–14 thomson. This fragmentation pattern is associated with the loss of CH_j ($0 \le j \le 2$) groups from the porphyrin ions. According to the present investigation the origin of the low-intensity peak structures in between the main fragments in the mass spectrum cannot be assigned unambiguously, i.e., fragmentation of the phenyl rings or a decomposition of the macrocycle. However, it is interesting to note that the first series of peaks centred at 649 thomson is 19 Da below the dominant $FeTPP^+$ ion. Moreover, the peak pattern of the first two series is similar to the $(FeTPP - P)^+$ cation whereas the two series of peaks at lower mass closely match the $FeTPP^+$ peak pattern.

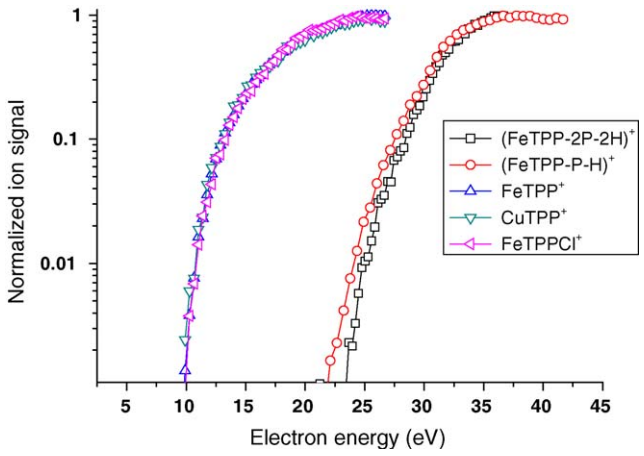

Fig. 5. Normalized ion efficiency curves of the most abundant singly charged fragment ions. The intersection of the curves with the x-axis is taken as the corresponding threshold energy (vanishing current method). The energy axis has been calibrated using argon as normalization standard, the presently determined appearance energy curves are thought to be accurate to approximately 0.5 eV. The electron current for these measurements is set to 10 μA to avoid artefacts such as multiple collisions with electrons.

3.2. Appearance energies

Fig. 5 shows ion efficiency curves for the major singly charged ions. The ion signal is measured as a function of the electron energy. The electron current is set to 10 μA to avoid artefacts such as multiple collisions with electrons. The threshold is determined by using a vanishing current method, i.e., the intersection of the measured curves with a line parallel to the x-axis at an ion yield that is three orders of magnitude lower than at 10 eV above the threshold. The accuracy of the presently determined appearance energy values is approximately 0.5 eV. It has to be mentioned that within this uncertainty the presently utilized method gives the same values as a more sophisticated procedure of fitting a Wannier threshold law to the data. After normalizing all the signals one can see that the appearance energies for the fragment $FeTPP^+$ with the mass to charge ratio 668 thomson, the parent $CuTPP^+$ (675 thomson), and the parent $FeTPPCl^+$ (703 thomson) are all about the same, around 9.7 eV. The present appearance energies are in general higher than the appearance energies obtained by Dale et al. [17] (using laser ionization techniques) or in comparison to photocurrent measurements in nonpolar solvents by Nakato et al. [18]. Both determine the appearance energy to be between 6.3 and 6.5 eV. The discrepancy may result from the different projectiles, i.e., photons and electrons. Whereas electron impact ionization almost exclusively gives the vertical ionization energy, photo ionization more likely reaches the adiabatic values via autoionization of a highly excited neutral intermediate state. It is interesting to

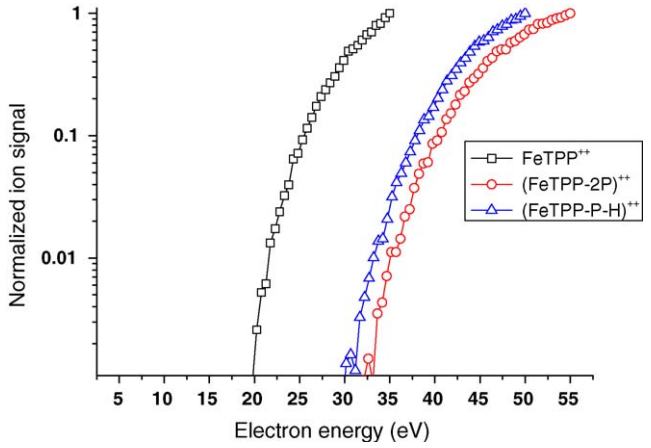

Fig. 6. Normalized ion efficiency curves of the most abundant doubly charged fragment ions. The intersection of the curves with the *x*-axis is taken as the corresponding threshold energy (vanishing current method). The electron current for these measurements is set to 10 μA to avoid artefacts such as multiple collisions with electrons.

note that according to the NIST database the ionization energy of the phenyl radical is 9.2 eV which is in good agreement to the presently determined ionization energies of the porphyrin parent ions. The fragments $(FeTPP - P)^+$ and $(FeTPP - 2P)^+$ both appear at approximately 20 eV. The dicationic parental ion could not be measured because the signal was too low. For the $FeTPP^{2+}$ (Fig. 6) we find an appearance energy of 18 eV and for the $(FeTPP - P–H)^{2+}$ and the $(FeTPP - 2P)^{2+}$ we observe an energy of 30 and 32 eV, respectively.

3.3. Metastable decays

In this work we also present results of an extensive study of decay reactions of the most prominent singly and doubly charged fragments. Decay reactions that take place in a metastable time regime can be investigated with the help of the so called MIKE scan technique [19]. With our modified three sector-field instrument [20] we have the possibility to check three different time windows in three different field-free regions. Fig. 7 shows MIKE spectra for the main decay reactions for singly charged ions. The upper panel shows the MIKE peak for the decay of the parent ion ($m/z = 703$) into the fragment ion with $m/z = 668$ thomson at a sector field voltage of 485.6 V. The narrow peak centred at the sector field voltage of 511 V is the corresponding parent peak. Please note that the yield of the fragment peak is multiplied by a factor of 100. The lower panel of Fig. 7 shows the MIKE peaks of the most abundant singly charged fragment ($m/z = 668$). The two MIKE peaks at sector field voltages 451.3 and 392.4 V correspond to the loss of one benzene molecule and a benzene molecule plus a phenyl group, respectively. The measurements that are shown, are recorded in the third field-free region to exclude interference with neighbouring isotopes of the ion under investigation.

Although one can observe the doubly charged parent FeTPPCl ion in the mass spectrum, the signal is too low for recording MIKE spectra. However, the signal is sufficient to observe metastable decay reactions of the dicationic FeTPP. In Fig. 8

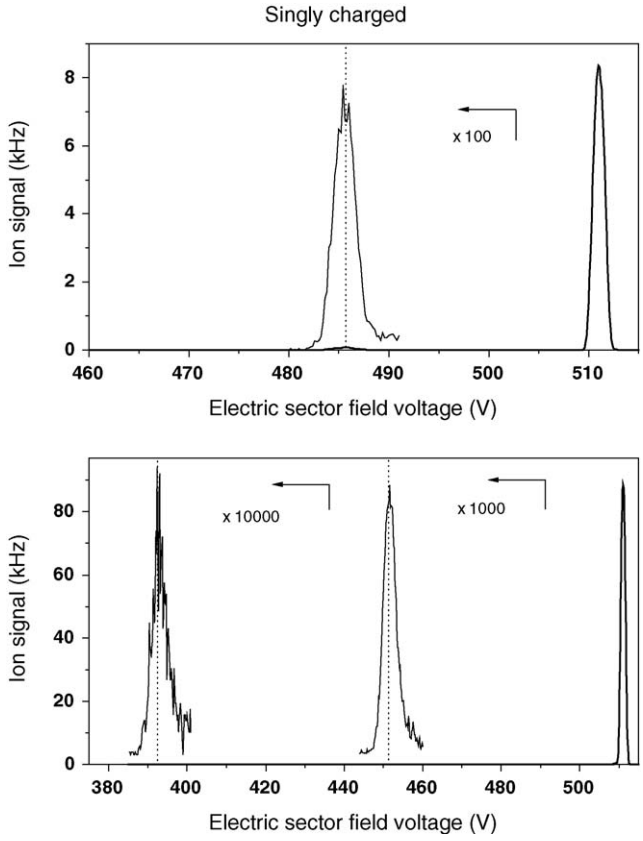

Fig. 7. MIKE spectra of selected singly charged ions. The narrow peaks at a sector field voltage of 511 V correspond to ions that pass through the instrument to the second electrostatic sector field (E2) without a delayed fragmentation. The peaks at lower sector field voltages are the result of unimolecular decomposition in ff3. The upper panel shows the metastable decay of the parent ion $FeTPPCl^+ \rightarrow FeTPP^+ + Cl$ with a <KER> of 171 meV. The dotted line indicates the expected position of the decay according to Eq. (1). The lower panel shows the metastable decay of $FeTPP^+ \rightarrow (FeTPP - P–H)^+ +$ neutrals and $FeTPP^+ \rightarrow (FeTPP - 2P–H)^+ +$ neutrals.

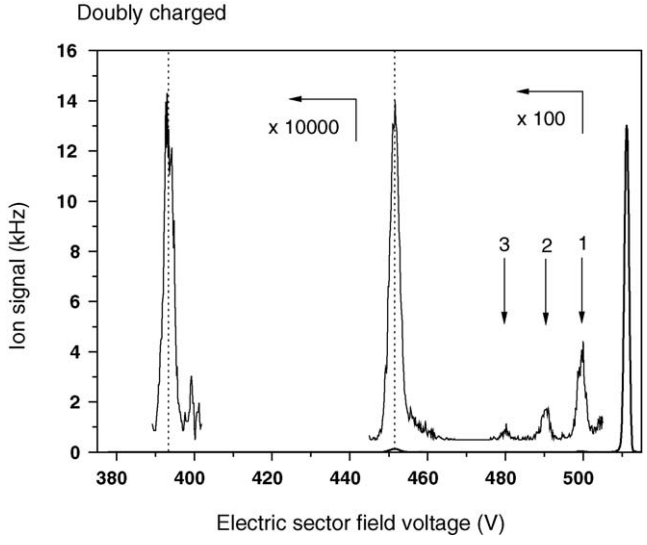

Fig. 8. MIKE spectra for the most abundant doubly charged fragment ions. The metastable $FeTPP^{2+}$ decays mainly into $(FeTPP - P–H)^{2+} +$ neutrals and with much lower intensity into $(FeTPP - 2P)^{2+} +$ neutrals. The peaks that are labelled with Arabic numbers correspond to the loss of low mass hydrocarbons containing 1–3 carbon atoms.

we present a MIKE spectrum of the FeTPP dication. Similar to the singly charged case, the ion with a mass of 668 Da ($m/z = 334$ thomson) decays into a doubly charged product ion with $m/z = 295$ (loss of benzene) and, in contrast to the singly charged case, into a dication with $m/z = 257$ (loss of two phenyl rings). Note that for better visibility the fragment peaks are multiplied by factors of 10^2 and 10^4, respectively. The peaks labelled with the numbers 1–3 correspond to the loss of masses 15.2 Da (probably a mixture of CH_3 and ($H + CH_3$, $H_2 + CH_2$) molecules), 27.3 Da (a mixture of C_2H_3 and C_2H_4 molecules) and 40.6 Da (a mixture of C_3H_4 and C_3H_5 molecules). The ratio of the intensity of the MIKE peaks of corresponding fragment and parent ions is a measure for the stability of the parent ion. For the doubly charged ions this so called metastable fraction is approximately 10 times higher compared to the corresponding singly charged ion and indicates a strongly reduced stability of the dications. Although a clear weakening of the porphyrin with increasing charge state is observed both in the mass spectra and the MIKE spectra no sign of a unimolecular charge separation reaction [21,22] has been observed in the present study.

From the shape of the MIKE peaks we have calculated a mean kinetic energy release <KER> of 171 meV for the decay of the parent ion $FeTPPCl^+$ into $Cl + FeTPP^+$. For the decay of the ion with $m/z = 668$ thomson into the fragment with $m/z = 590$ thomson we deduce a <KER> of 185 meV. The $(FeTPP - Cl)^{2+}$ decays into $m/z = 295$ thomson via the release of 209 meV kinetic energy (based on the assumption that the parent splits into one charged and only one neutral fragment).

Acknowledgements

This work was partly supported by the FWF, Wien, and the European Commission, Brussels (network program) and has been performed within the Association EURATOM-ÖAW. The content of this publication is the sole responsibility of its publishers and it does not necessarily represent the views of the EU Commission or its services. F.Z. gratefully acknowledges a pos-doc grant from the Brazilian agency CNPq. We thank Prof. D. K. Böhme for many stimulating discussions and for critical reading of the manuscript.

References

[1] A.R. Battersby, Pure Appl. Chem. 65 (1993) 1113.
[2] K.M. Kadish, K.M. Smith, R. Guilard (Eds.), The Porphyrin Handbook, vols. 1–10, Elsevier Science, Oxford, 2000;
K.M. Kadish, K.M. Smith, R. Guilard (Eds.), The Porphyrin Handbook, vols. 11–20, Elsevier Science, Oxford, 2003.
[3] B. Kräutler, Chimia 41 (1987) 277.
[4] D.R. Doiron, C.J. Gomer (Eds.), Porphyrin Localization and Treatment of Tumors, A. R. Liss, New York, 1984.
[5] D.L. Drabkin, in: D. Dolphin (Ed.), The Porphyrins, vol. I, Wiley, New York, 1978, p. 29.
[6] D. Gust, T.A. Moore, Science 244 (1989) 35.
[7] J. Deisenhofer, H. Michel, Angew. Chem. Int. Ed. Eng. 101 (1989) 872.
[8] H.J. Callot, R. Ocampo, Geochemistry of porphyrins, in: K.M. Kadish, K.M. Smith, R. Guilard (Eds.), The Porphyrin Handbook, vol. 1, Elsevier Science, Oxford, 2000, p. 349.
[9] E.W. Baker, J.W. Louda, in: R.B. Johns (Ed.), Biological Markers in the Sedimentary Environment, Elsevier, Amsterdam, 1986, p. 125.
[10] J.F. Branthaver, R.H. Filby, Metal Complexes in Fossil Fuels, American Chemical Society, Washington, DC, 1987, p. 84.
[11] J.S. Lindsey, Synthesis of meso-substituted porphyrins, in: K.M. Kadish, K.M. Smith, R. Guilard (Eds.), The Porphyrin Handbook, vol. 1, Elsevier Science, Oxford, 2000, p. 445.
[12] J.M.E. Quirke, Mass spectrometry of porphyrins and metalloporphyrins, in: K.M. Kadish, K.M. Smith, R. Guilard (Eds.), The Porphyrin Handbook, vol. 7, Elsevier Science, Oxford, 2000, p. 371.
[13] S. Matt, M. Sonderegger, R. David, O. Echt, P. Scheier, J. Laskin, C. Lifshitz, T.D. Märk, Int. J. Mass. Spectrom. 187 (1999) 813.
[14] S. Matt-Leubner, A. Stamatovic, R. Parajuli, P. Scheier, T.D. Märk, O. Echt, C. Lifshitz, Int. J. Mass. Spectrom. 222 (2003) 213.
[15] K. Gluch, J. Fedor, S. Matt-Leubner, O. Echt, A. Stamatovic, M. Probst, P. Scheier, T.D. Märk, J. Chem. Phys. 118 (2003) 3090.
[16] J.D. Laycock, J.A. Ferguson, R.A. Jost, J.M.E. Quirke, A. Rohrer, R. Ocampo, H. Callot, J. Mass Spectrom. 32 (1997) 978.
[17] M.J. Dale, K.F. Costello, A.C. Jones, P.R.R. Langridge-Smith, J. Mass Spectrom. 31 (1996) 590.
[18] Y. Nakato, K. Abe, H. Tsubomura, Chem. Phys. Lett. 39 (1976) 358.
[19] S. Feil, K. Gluch, P. Scheier, K. Becker, T.D. Märk, J. Chem. Phys. 120 (2004) 11465.
[20] S. Matt-Leubner, A. Stamatovic, R. Parajuli, P. Scheier, T.D. Märk, O. Echt, C. Lifshitz, Int. J. Mass Spectrom. 222 (2003) 213.
[21] P. Scheier, T.D. Märk, Phys. Rev. Lett. 73 (1994) 54.
[22] P. Scheier, B. Dünser, T.D. Märk, Phys. Rev. Lett. 74 (1995) 3368.